UV-Vis Spectrometric Quantification of Nitric Oxide Production by the Anticancer Drug Suberoylanilide Hydroxamic Acid (SAHA, Vorinostat).

by

Ishita Patel

May, 2011

A thesis submitted to the Graduate Faculty of

The Biomedical Sciences Department

SCHOOL OF HEALTH PROFESSIONS AND NURSING

LONG ISLAND UNIVERSITY, C.W. POST CAMPUS

In partial fulfillment of the requirements for the degree of Master of Science in Medical Biology with specialization in: Medical Chemistry.

Approved

Prof. Uri Samuni (Mentor)

Prof. Paul Dominguez (Member)

Prof. Anthony Capetandes (Member)

LONG ISLAND UNIVERSITY, C.W. POST CAMPUS
SCHOOL OF HEALTH PROFESSIONS AND NURSING
BIOMEDICAL SCIENCES DEPARTMENT

****

A thesis submitted to the Graduate Faculty

Date: April 29, 2011

This is to certify that Ishita Patel has successfully completed all requirements for the MASTER OF SCIENCE DEGREE in

Medical Chemistry

Thesis Title: Nitric Oxide Production by SAHA

Preparation of Thesis Proposal and Experimental Research Thesis: BMS 703 & 708

Approved

Prof. Uri Samuni (Mentor)

Prof. Paul Dominguez (Member)

Prof. Anthony Capetandes (Member)

TABLE OF CONTENTS

ACKNOWLEDGEMENT

I would like to express my sincere gratitude to my advisor Prof. Uri Samuni for the continuous support of my Master's research, for his patience, motivation, enthusiasm, and immense knowledge. His guidance helped me in all the time of research and writing of this thesis.

Besides my advisor, I would like to thank the members of my thesis committee: Prof. Anthony Capetandes, and Prof. Paul Dominguez, for their encouragement, insightful comments, and more importantly, making the completion of this thesis even more challenging.

My sincere thanks also go to Prof. Jorge Ramos, for his constructive and sometimes destructive criticism of the experimental protocols, presentation of the data, and writing style.

I would like to acknowledge and extend my heartfelt gratitude to my parents Umesh Patel and Shobha Patel, for supporting me spiritually throughout my life.

Last but not least I would like to thank my brother Vipul Patel and my good friend Jignesh Patel for their financial support, encouragement, and help during difficult times.

ABSTRACT

UV-Vis Spectrometric Quantification of Nitric Oxide Production by the Anticancer Drug Suberoylanilide Hydroxamic Acid (SAHA, Vorinostat).

by

Ishita Patel

We have monitored Nitric Oxide (NO) production by Suberoylanilide Hydroxamic Acid (SAHA, vorinostat), using UV-Vis Spectrometry. SAHA is known to cause growth arrest and death of a broad variety of transformed cells both *in vitro* and *in vivo* at concentrations not toxic to normal cells. With its role as a pleiotropic regulator, NO is critical to numerous biological processes of interest for cancer research, including macrophage-mediated immunity. Our results indicate that SAHA has the slowest NO production rate despite being the best anticancer drug of the compounds studied. The conclusion is that NO production is not the primary function of SAHA. Its main function is Histone deacetylase inhibition and the relatively slow NO release rate means that SAHA is more resistant to oxidation than the other compounds studied. That would enable SAHA to remain in the body for longer periods of time, requiring fewer doses of the drug to be administered to cancer patients.

Our research employed a NanoDrop Spectrometer and we found the reproducibility of Optical Density (O.D.) readings to be quite good. The sample volumes were as low as 200 µL and this was enough for taking multiple readings. This type of instrument would be a good choice for studying samples that are expensive or in short supply such as the anticancer drug SAHA.

LIST OF ILLUSTRATIONS

LIST OF TABLES

CHAPTER I INTRODUCTION

1.1 Histone deacetylases as therapeutic targets

The expression of genes is regulated, in large part, by the structure of the chromatin proteins around which the DNA is wrapped. The basic repeating unit of chromatin is the nucleosome, composed of DNA wrapped around the histone octamer composed of two copies of each of four histones, H2A, H2B and H3 and H4.[1] Mechanisms of gene transcription involve the reversible post-translational modification of amino acids in the histone tails by acetylation of lysines and arginines. [2,3]

Histone deacetylases (HDACs) are a family of enzymes comprising nuclear repressor complexes involved in the regulation of gene expression, DNA repair, and stress response. A simplified mechanism proposes that the repressor complexes maintain nucleosome histones in a state of deacetylation, limiting transcription factor access to DNA [Figure 1.1]. Normally, the positively charged amine groups on lysine and arginine amino acids allow histone tails to interact with and bind to the negatively charged phosphate groups on the DNA backbone. The positive charges on the histone are neutralized by changing amines into amides. This modification decreases the ability of the histones to bind to DNA and allows chromatin expansion. HDACs remove those acetyl groups, resulting on increased DNA binding, which results in a condensed DNA structure not viable for the transcription process to take place. Such processes often are altered in tumors, and empirical observations suggest that HDAC activity is increased in cancer cells resulting in altered gene transcription and increased cell survival. [4]

Cancer in general is the result of epigenetic alterations and consequentially can be targeted by epigenetic therapies such as HDAC inhibition. Such inhibitors possess

antitumor activity at concentration that are well tolerated by normal cells, supporting the idea that their use might develop as a specific strategy for cancer treatment. [5,6] HDAC inhibitors have had pronounced antitumor activity with promising results in clinical trials. The molecular basis for their selective antitumor activity is, however, unknown.

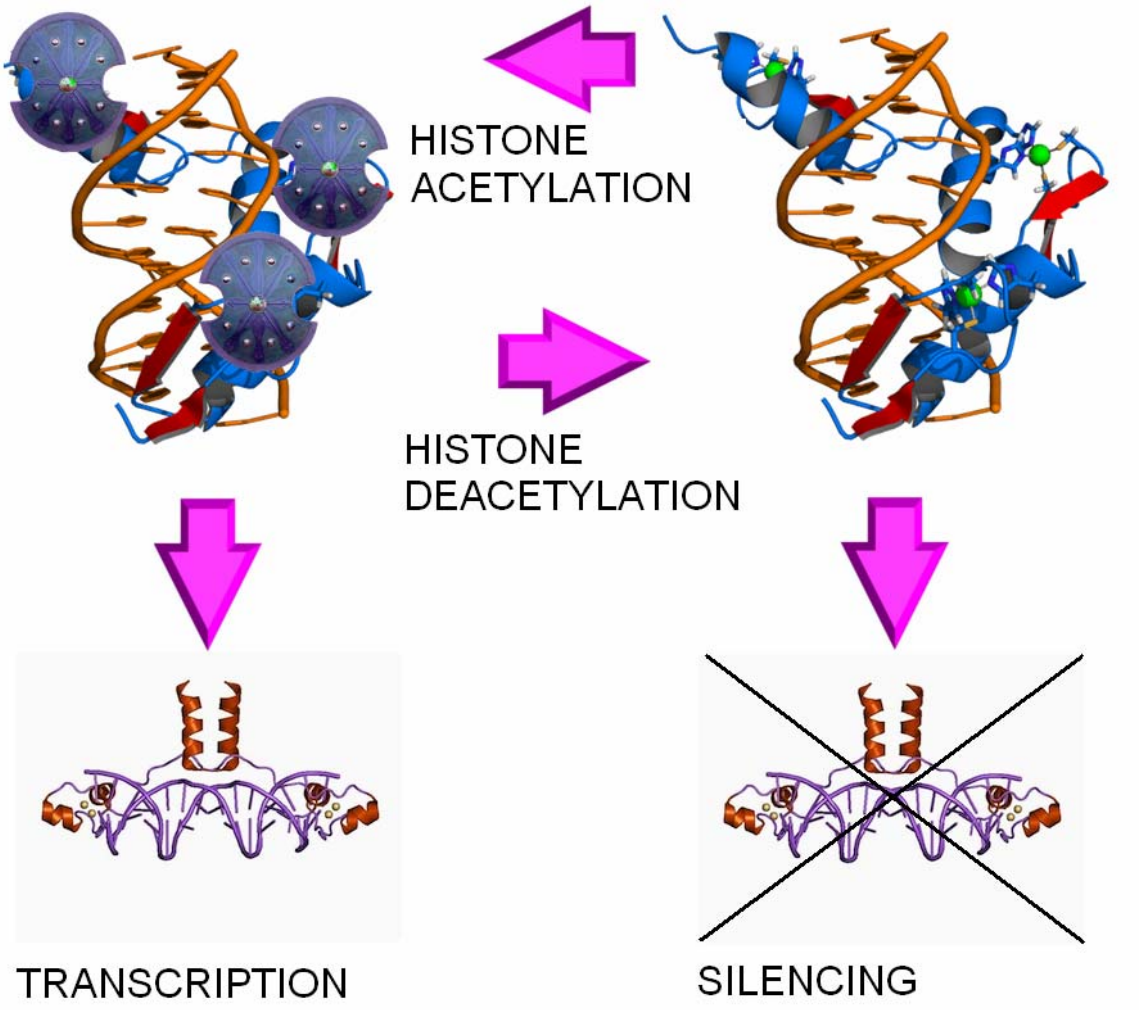

Figure 1.1. Histone deacetylase inhibition. Nucleosomal histones are subject to acetylation (acetyl groups represented by shields) by histone acetyltransferases. HDACs remove those acetyl groups, leaving positively charged amine groups on lysine and arginine (positively charged groups in green). Hyperacetylated chromatin is transcriptionally active, and hypoacetylated chromatin is silent.

1.2 Hybrid polar compounds and possible mode of action

Hexamethylene bisacetamide (HMBA), and its structural analogs are called hybrid polar compounds (HPCs) because they have in common two polar groups separated by an apolar 5- to 6-carbon methylene chain. HMBA is a low molecular weight synthetic compound, induces terminal differentiation and apoptosis in transformed cells in culture. Since the inhibition of physiologic cell death is one of the main factors that contribute to the spread of cancer, HMBA was once viewed as a suitable anticancer agent. [7,8] The idea was abandoned because of its toxicity and the relatively high dosage required for the compound to have a significant effect.

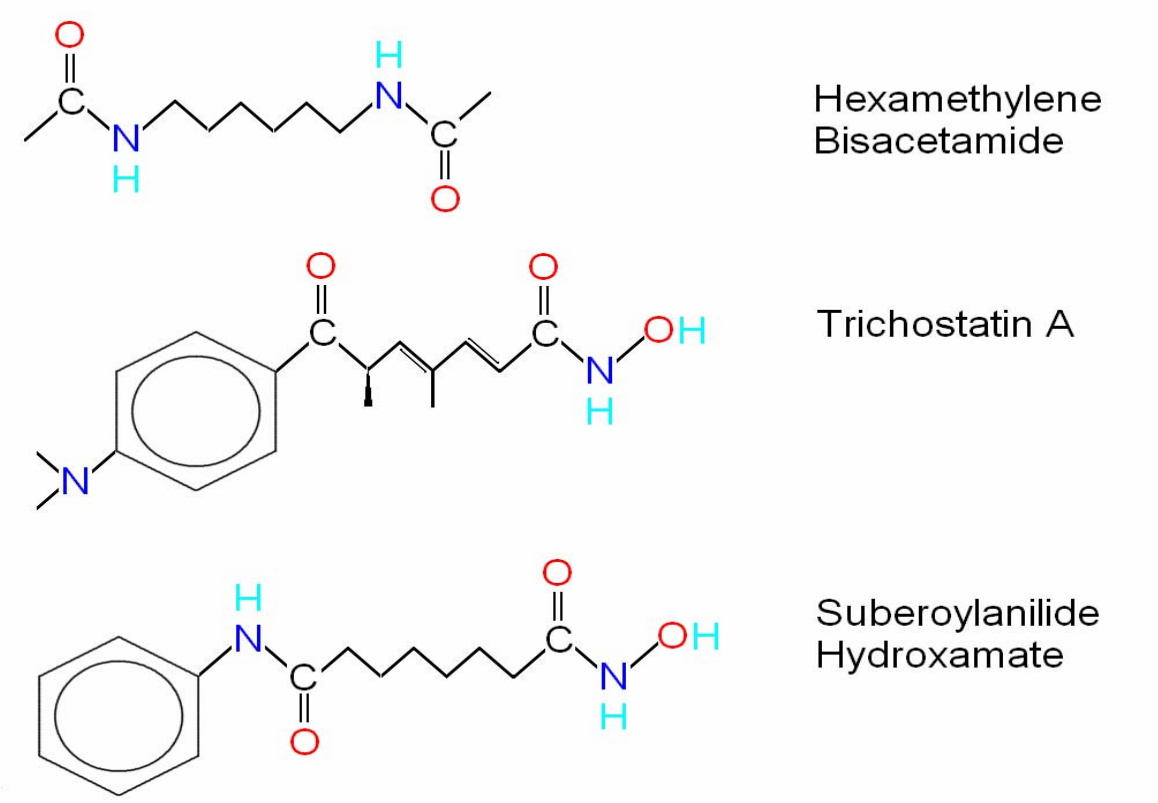

Figure 1.2. Chemical structures of Hexamethylene bisacetamide (HMBA), Trichostatin A (TSA), and Suberoynilide Hydroxamate (SAHA).

Compounds structurally related to, but more potent than, HMBA represent a relatively new group second generation HPCs which show significant activity against a broad spectrum of neoplasms, at doses that are not toxic to cancer patients. Suberoynilide Hydroxamate (SAHA) is one of the HPCs most advanced in development. The structure of SAHA is related to that of trichostatin A (TSA) [Figure 1.2]. The rationale behind the synthesis of SAHA is that a hydrophobic phenyl group at one end of the molecule might enhance its activity. SAHA is a potent inducer of cell differentiation and an inhibitor of HDAC activity. [9,10]

Second generation HPCs inhibit HDACs activity at or below micromolar concentrations, both in vitro and in vivo. X-ray crystallographic analyses of human HDAC8 in complex with a hydroxamic acid inhibitor, showed that the catalytic site of the enzyme has a tubular pocket with a zinc-binding site at its base. [11, 12] The polar component (hydroxamic moiety) of TSA and that of SAHA were shown to bind to the zinc at the base of the active site. The carbon ring of these compounds projects out of the pocket onto the surface of the protein and is thought to provide additional stability to the protein-inhibitor complex. [13] Although the inhibition mechanism of second generation HPCs is not well understood, the structural analogs of SAHA have the requirements for binding the zinc in the active site of HDAC8 and block access to the channel leading to the catalytic site. The structural analogs, in summary, have a cap group that interacts with the rim of the catalytic tunnel, a hydrophobic spacer to allow the molecule to lie into the tunnel, and a zinc-binding group to complex the zinc ion at the bottom of the catalytic cavity. [Figure 1.3]

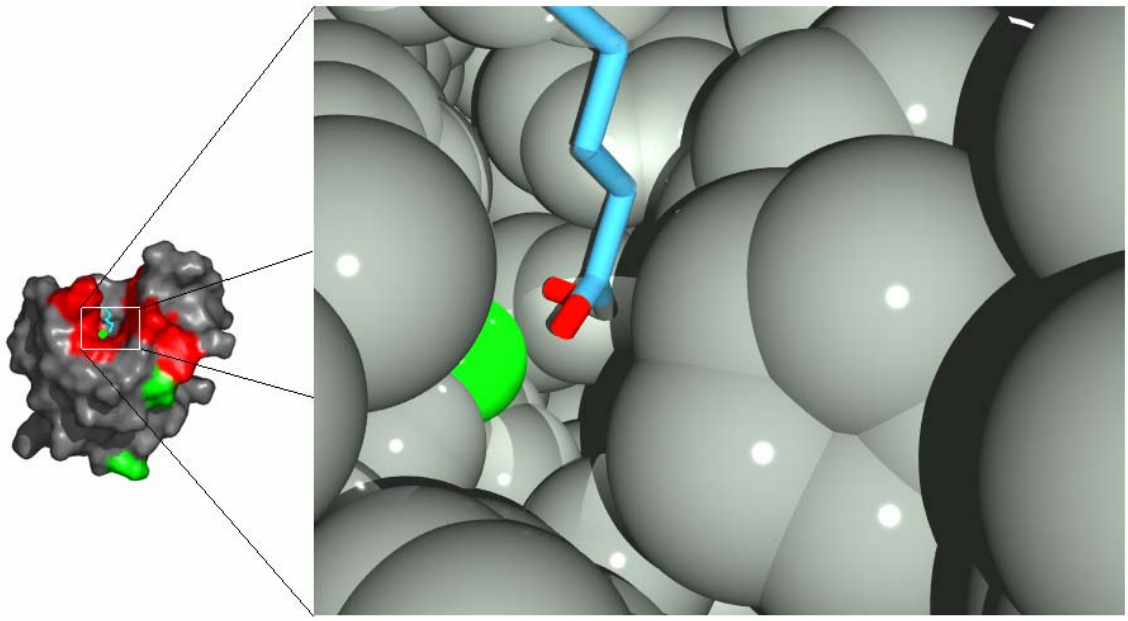

Figure 1.3. Zinc-dependent histone deacetylase, human HDAC8, complexed with a SAHA structural analog. The zinc atom has been drawn as a green sphere, the SAHA structural analog has been drawn as a stick figure with the hydrophobic spacer colored aqua and the hydroxamic moiety colored in CPK code.

1.3 The role of Nitric Oxide in cancer

As a therapeutic agent, the use of nitroglycerin had been documented as early as 1879. That is, even before it was determined that NO was the molecular species at work [14] Recently, NO has been shown to be involved in the anti-pathogen and anti-tumor host response and other autoimmune processes. Because of its variety of reaction partners and concentration-dependent activity, the function of NO in the immune system cannot yet be fully explained. [15,16] It has been observed that increases or decreases in NO levels might be therapeutically desirable. However, the wide range of processes in which NO has been implicated pose considerable challenges for drug development. Since protective and toxic effects of NO are frequently seen in parallel, pharmacologically modulating NO levels is still a therapeutic wild card. [Figure 1.4]

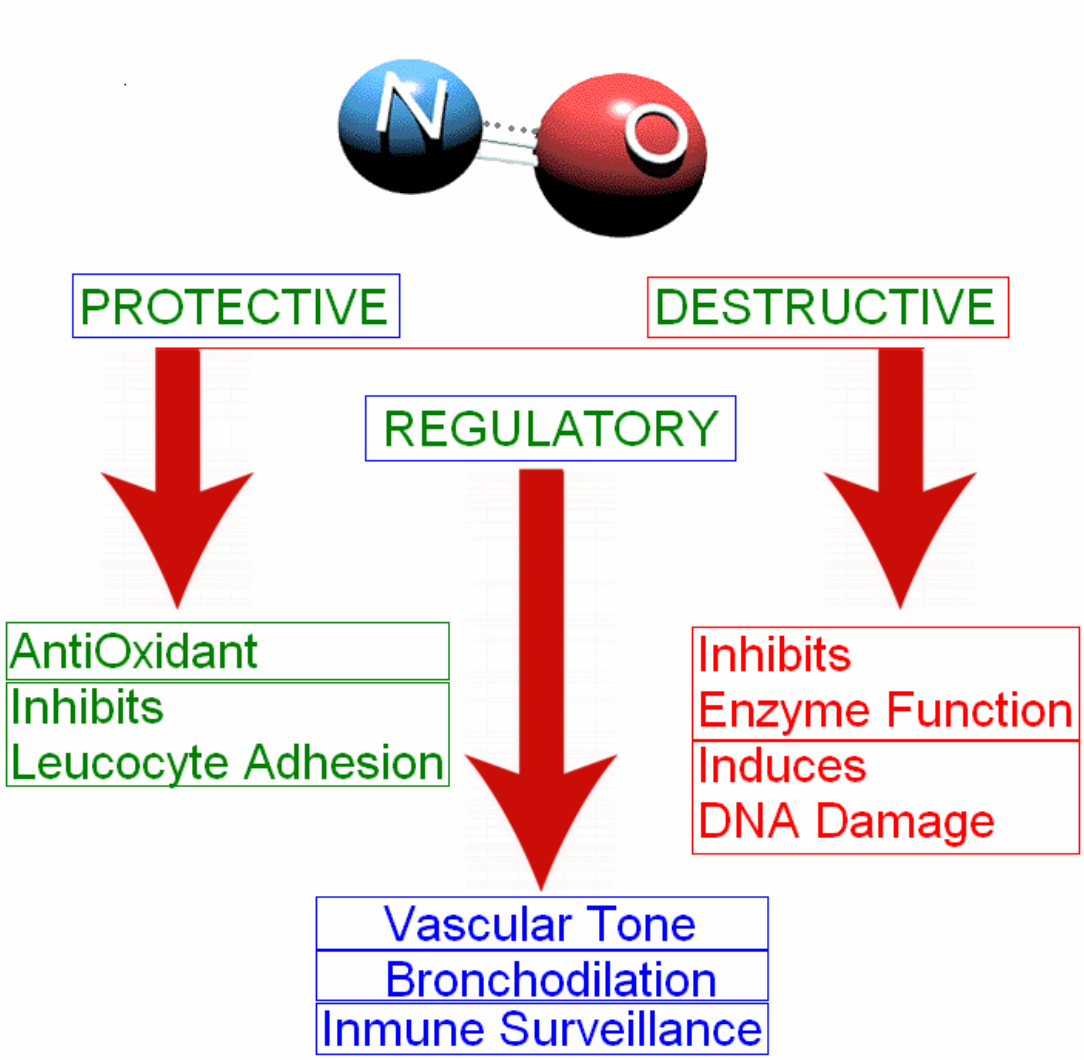

Figure 1.4. Various biological effects of Nitric Oxide.

A good starting point in understanding the function of NO in mammalian physiology is to categorize its chemical effects as two distinct classes; direct and indirect. The direct effects are the result of NO interaction with biological molecules, as opposed to indirect effects, which are the result of the action of reactive nitrogen oxide species and other NO derivatives. [17] NO is naturally generated within mammalian cells by a family of Nitric Oxide Synthases (NOS) enzymes, most notably the inducible Nitric Oxide

Synthase (iNOS). The NO generated by iNOS exhibits anti-tumour activity. Various direct and indirect mechanisms have been proposed to explain the anti-tumour properties of NO, including direct damage of DNA and inhibition of DNA synthesis. [18]

1.4 Research goals and the subject of this thesis

The source for anticancer activity of SAHA and its structural analogs is still under investigation. It is well known that these compounds are capable of NO production but there is no clear cut explanation as to the role of NO in the regulation of carcinogenic process. Nevertheless, different studies have concluded that NO production might affect cancer cells in a way that increases their death rate or otherwise exerts an anticancer effect. Some of the unanswered questions related to the therapeutic use of SAHA and its structural analogs include whether the rate of NO production directly related to the anti-cancer activity of SAHA and its structural analogs; and what chemical or structural features make an HPC better as an anti-cancer drug.

The above topics are beyond the scope of this thesis, which will attempt to establish a working procedure and experimental set up for studying the rate of NO release from HPCs upon oxidation and answer the following, simpler questions:

[1] What is the rate of NO release upon oxidation by metMb/H_2O_2 for each of the HPCs that were used?

[2] What structural and chemical features of the different HPCs make these rates different?

[3] How reproducible are the measurements of the NanoDrop Spectrometer? Is this the best way to analyze small samples of hard to obtain chemicals?

CHAPTER II MATERIALS AND METHODS

2.1 Reagents and Instruments

Spectroscopic measurements were carried out using a HP8453 diode array spectrometer from Agilent Technologies (Plateau time for Griess Assay) and a NanoDrop Spectrometer 2000 from Thermo Scientific (everything else).

All chemicals were of the highest purity available. The table below summarizes the reagent properties and form of stock solution preparation.

Solution and Concentration	Source and CAS Number		Form of Preparation
0.495 mM Met Myoglobin	Sigma Aldrich >90% purity **100684-32-0**		100 mM Phosphate buffer (pH 6.5) was saturated with Met Myoglobin from horse heart (Sigma Code M-1882). Solution was filtered through a Sephadex column, bead size 20-80 microns
3000 units/mL Catalase from Bovine Liver	Sigma Aldrich Unknown Purity **9001-05-2**		3.0 mg of Catalase per 1.0 mL Phosphate buffer (pH 7.4)
1.0 M Hydrogen Peroxide	J.T. Baker 30% Purity **7722-84-1**		Dilute 1.0 ml of 10 M reagent grade hydrogen peroxide to 10.0 mL Volume By adding DI Water.
100 mM Sodium Nitrite	Sigma Aldrich >97% Purity **7632-00-0**		Dissolve 69.0 mg Sodium Nitrite in 10.0 mL DI water
1% NEDD (Griess **Solution A**)	Sigma Aldrich Unknown Purity **1465-25-4**		1.0 mg NEDD per 1.0 mL DI Water
2% Sulfanilamide (Griess **Solution B**)	Sigma Aldrich Unknown Purity **63-74-1**		20 mg Sulfanilamide per 1.0 mL of 5% HCl
25 mM Acetohydroxamic acid	Sigma Aldrich 98% Purity **546-88-3**		34.3 mg of Acetohydroxamic acid in 10.0 mL DI water
25 mM Benzohydroxamic acid	Sigma Aldrich 99% Purity **495-18-1**		34.3 mg of Acetohydroxamic acid in 10.0 mL DI water.
10 mM (SAHA) Suberoylanilide Hydroxamic Acid	Merck and Co. Unknown Purity **149647-78-9**		2.64 mg SAHA per 1.0 mL Dimethyl Sulfoxide (DMSO)

Table 2.1. Summary of Stock solutions used, including source and CAS number for all chemicals.

2.2 Nitrite extinction coefficient from Griess Assay

NO has a half-life of less than 30 seconds, and reacts rapidly with free oxygen, oxygen radicals, redox metals, sulphydryls, disulfides and oxygenated hemoglobin. [19] The stable degradation products of NO, nitrite (NO_2^-) and nitrate (NO_3^-), accumulate in solution and can be measured using the Griess reaction. The detection limit of the technique is in the micromolar range and the concentrations of nitrite and nitrate can be assessed as an index of NO production. The Griess reaction is based on the two-step diazotization reaction in which acidified NO_2^- produces a nitrosating agent which reacts with sulfanilic acid to produce the diazonium ion. [20] This ion is then coupled to N-(1-naphthyl) ethylenediamine to form the chromophoric azo-derivative which absorbs light at 540 nm [Figure 2.1].

The concentrations of nitrite were determined by comparison to a standard curve, constructed using sodium nitrite ranging from 20 to 250 µM [Table 2.1]. Each assay used to prepare the standard curve contains 200 µL of the diluted sodium nitrite, 100 µL of Solution A and 100 µL of solution B. Each point on the standard curve is an average of three trials. This average value was taken as an approximation of the Nitrite extinction coefficient. The extinction coefficient from the best fit line (average) is **0.0051 μM^{-1}.** This value is in excellent agreement with the one we computed using the sample data from the Parameter™ Griess Reagent Protocol documentation (R&D Systems, Inc.). The value obtained from that source is between 0.0049 and 0.0050 **μM^{-1}.** [21] Our results also agree with similar measurements on the spectrometric determination of Nitrite and Nitric Oxide in furnace atmospheres during the late 1930's. [22]

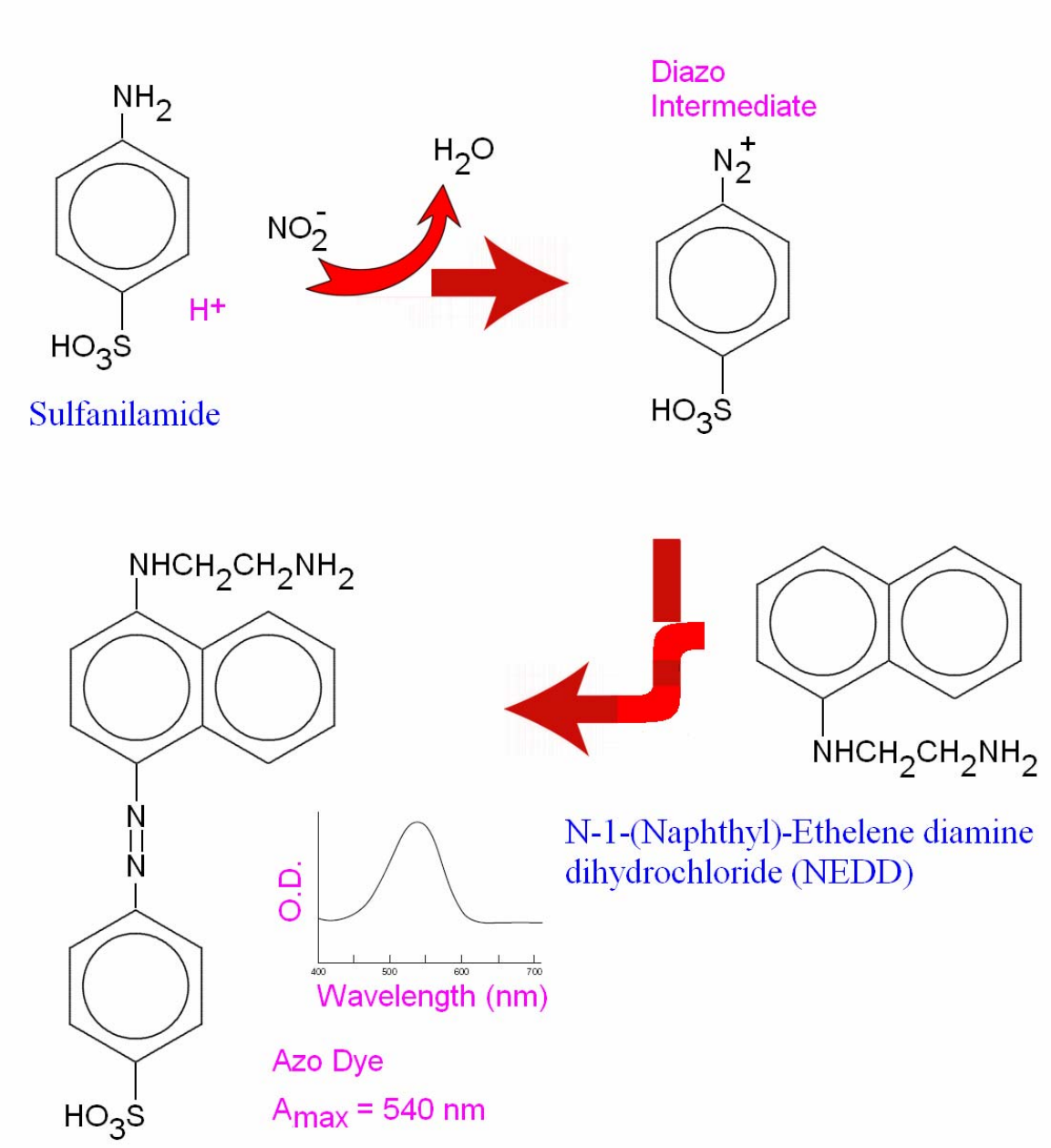

Figure 2.1. Schematics of the Griess Reagent System, which uses sulfanilamide and *N*-1-napthylethylenediamine dihydrochloride (NEDD) under acidic conditions to detect the stable degradation products of NO, nitrite (NO_2^-) and nitrate (NO_3^-).

Trial 1	Trial 2	Trial 3	Aver	Nitride Concentration
O.D.	O.D.	O.D.	O.D.	(μM)
0.133	0.264	0.169	0.189	20
0.194	0.317	0.243	0.251	30
0.248	0.375	0.304	0.309	40
0.305	0.416	0.367	0.363	50
0.575	0.700	0.637	0.637	100
0.796	0.925	0.920	0.880	150
1.014	1.174	1.135	1.108	200
1.264	1.413	1.415	1.364	250

Table 2.2. Sodium Nitrite concentrations and respective O.D. readings used to build the standard curve. Each O.D. in a trial is an average of two readings. The O.D. was measured at 540 nm within 30 min after the reactants were mixed.

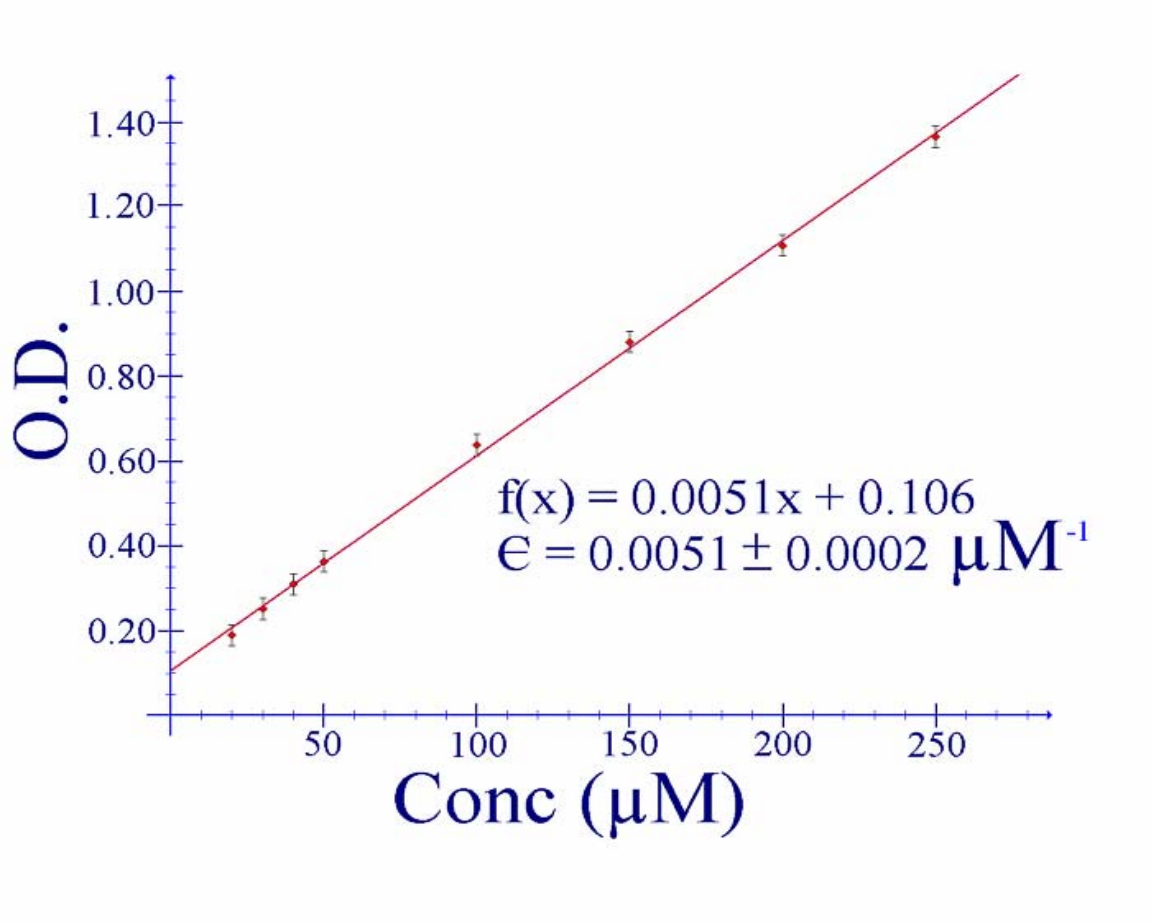

Figure 2.2. Standard curve used to convert the O.D. readings into concentrations of the stable degradation products of NO, nitrite (NO_2^-) and nitrate (NO_3^-). The standard curve was build from the average of three trails. The extinction coefficient from the best fit line (average) is **0.0051 μM^{-1}.**

2.3 Nitrite Detection Plateau Time

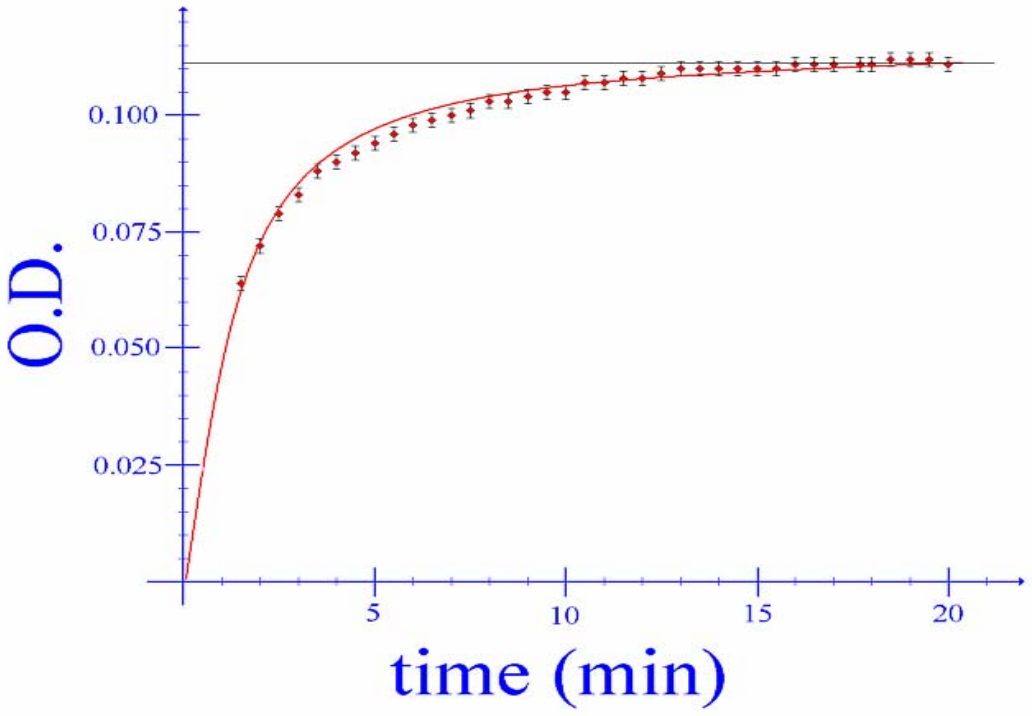

Figure 2.3. O.D. as a function of time for the Griess Assay, prepared by mixing 500 µL of 100 µM sodium nitrite, 250 µL of Solution A and 250 µL of solution B.

The first step of the research project was to figure out the time at which the reaction reaches the steady state level. For that end we mixed 500 µL of 100 µM sodium nitrite, 250 µL of Solution A and 250 µL of solution B. The change in O.D. was measures at 540 nm using a HP8453 diode array spectrometer from Agilent Technologies. The result (**Figure 2.3**) indicates that the color of the Azo dye will be fully developed after 20 minutes. The R&D Systems, Inc. protocol suggests that the measurements be done within one hour, after which time the azo dye will start degrading into colorless byproducts [21] We noted that if the color evolution of the Griess assay is followed beyond the 20 minute plateau time the O.D. will start to fluctuate and eventually decrease (results not shown).

2.4 NO production: Oxidation of Hydroxamides

The reaction assays were prepared as listed on **Table 2.3**. First we put 700 µL Phosphate buffer (pH 7.4) into a 1 mL centrifuge tube. Then we add 100 µL of each reagent: 2.5 mM Hydroxamide compound, 100 mM Met Myoglobin, and 50 mM H_2O_2. The Met Myoglobin (Fe^{3+}) reacts with hydrogen peroxide to yield the oxo-ferryl species (Fe^{4+}=O), which oxidizes the hydroxamide substrate (**Figure 2.4**). [23] We take time 0 minutes as the instant when the last of the three reagents is added to the centrifuge tube. The reaction is stopped by withdrawing 100 µL from the reaction assay and mixing with 50 µL of 300 units/mL catalase (**See section 2.5**) which has been previously put into the centrifuge tube. Then we add 50 µL of Griess reagents A and 50 µL of Griess reagent B within seconds of each other. The samples were then analyzed in the NanoDrop Spectometer within 30 minutes.

Note that the concentration of the reagents in the reaction mixture is not the same as their concentration in the samples taken to the NanoDrop. The samples contain 100 µL from the reaction assay, 50 µL of Griess reagents A, 50 µL of Griess reagent B, and 50 µL of 300 units/mL catalase. Thus the sample volume is 250 µL to give a dilution factor of **2.5**, which is factored in when computing NO production rates. For example, if we get for SAHA 0.0018 O.D. per min,

$\Delta C = \Delta OD \div \varepsilon \rightarrow$ Delta C(µM per min) = 0.0018 O.D. per min $\div$ 0.0051 μM^{-1}
ΔC = 0.353 µM per min $\rightarrow$ X 2.5 Volumes = 0.882 µM per min

Here we have used Beer-Lambert's law to convert the rate of change in O.D. to the rate of change in units of concentration (µM). Then we used the 2.5 dilution factor to compute the NO concentration in the reaction assay.

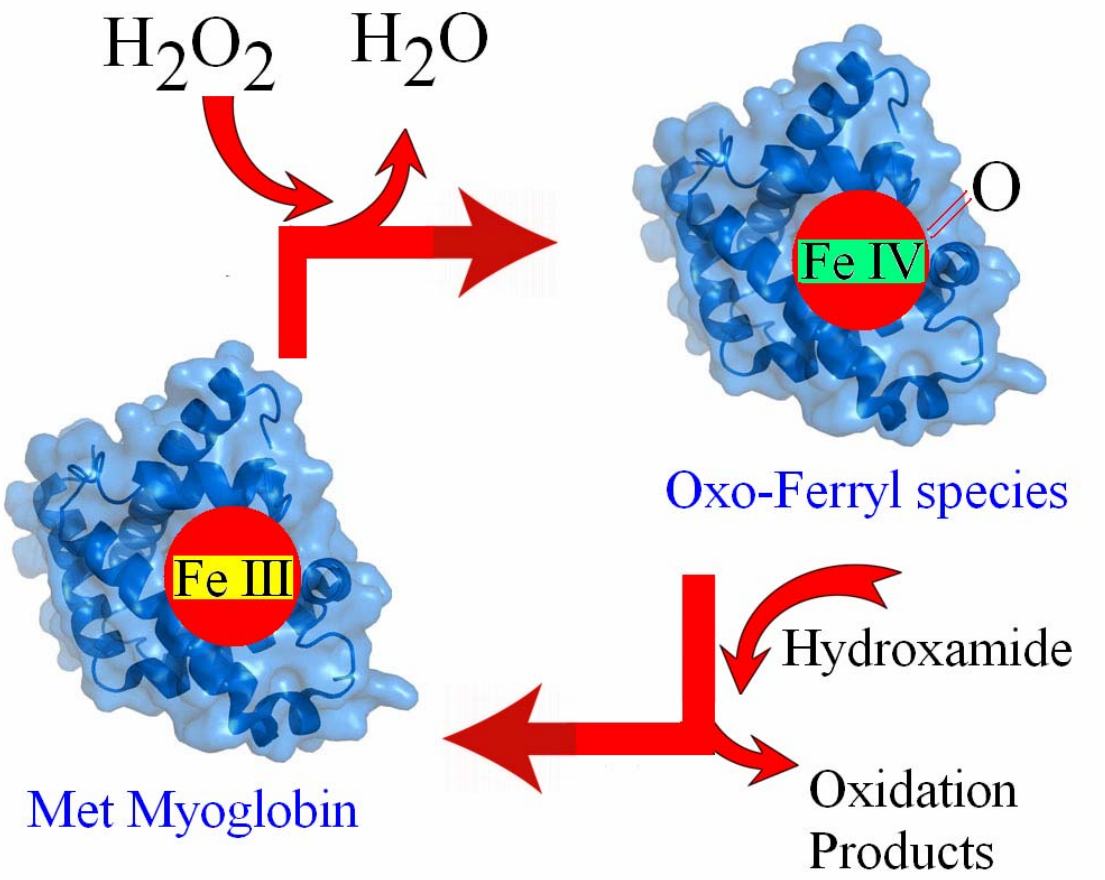

Figure 2.4. ReDox cycle where Met Myoglobin (Fe^{3+}) reacts with hydrogen peroxide to yield the oxo-ferryl species (Fe^{4+}=O), which oxidizes the hydroxamide substrate.

Reagent and Initial Concentration	**Volume (µL)**	**Final Concentration (µM)**
2.5 mM AcetoHydroxamic Acid 2.5 mM Hydroxy Urea	100	250
2.5 mM BenzoHydroxamic Acid	100	250
2.5 mM Suberoylanilide Hydroxamic Acid	100	250
50 mM H_2O_2	100	5000
100 mM Met Myoglobin	100	10

Table 2.3. Concentrations of reagents in the reaction assay. The solutions were mixed and diluted to 1000 µL (1 mL) by adding Phosphate buffer (pH 7.4). The final concentration of each reagent takes into account this dilution factor (1:10).

2.5 Catalase Activity Assesment

We found it nesesary to use a quencher to stop the hydroxamide oxidation reaction at different time points. According to **Figure 2.4**, the reaction can be stopped while the hydroxamide is still in the solution if the Met Myoglobin (Fe^{3+}) is not converted into the oxo-ferryl species (Fe^{4+}=O). This step of the reaction requires H_2O_2. Thus we used the enzyme catalase to deplete the H_2O_2 and stop the reaction.

The enzymatic activity of catalase from bovine liver, Sigma code C9322, was tested by following the decomposition of H_2O_2 at 240 nm, where H_2O_2 has an extinction coefficient of 43.6 $M^{-1}cm^{-1}$. We carried out the kinetic measurement with 900 µL of 25 mM concentration of H_2O_2 and 100 µL 3.0 X 10^{-2} mg/mL Catalase prepared by successive dilution of the stock solution listed on **Table 2.1**. This gives a 1 mL assay with working concentration of 22.5 mM H_2O_2 and 100 µL 3.0 X 10^{-3} mg/mL Catalase.

The reaction was followed during the first 2 minutes in the Diode array and during the first 5 minutes on the NanoDrop spectrometer. Because the solution could not be removed once the kinetic measurement was started in the diode array, the reaction rate seems to slow down if allowed to go for long periods of time. We think that the H_2O_2 concentration was high enough at all times of the measurement to assume that the reaction rate is zero order with respect to H_2O_2. The reaction rate seems to remain steady for a longer period of time during the NanoDrop measurements because the solution is constantly being mixed. No bubbles were observed when using a catalase concentration of 3.0 X 10^{-3} mg/mL. Bubbles were observed using a catalase concentration of 3.0 X 10^{-2} mg/mL.

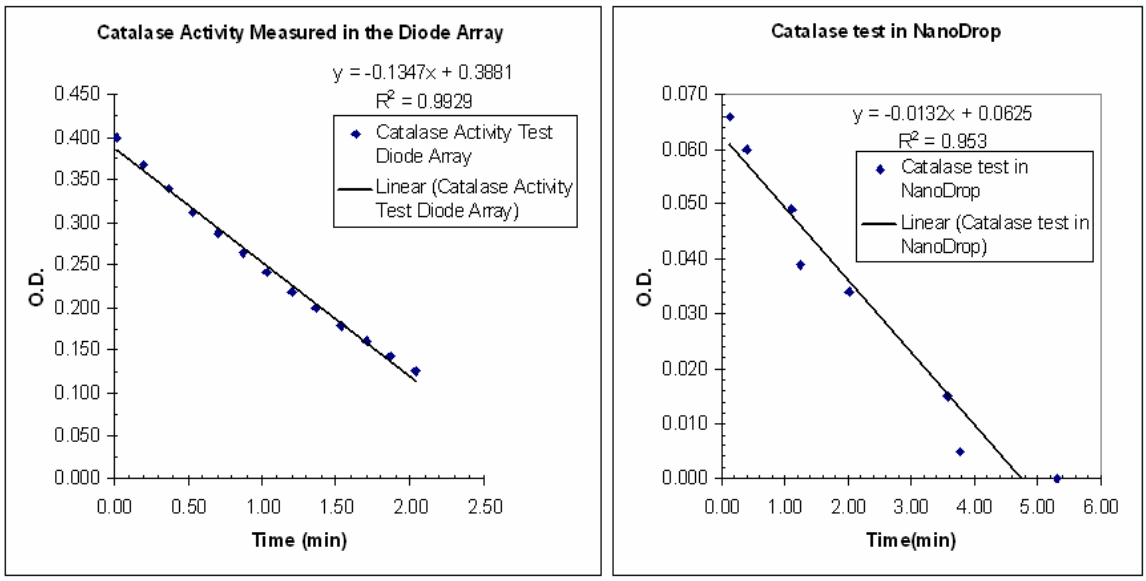

Figure 2.5. Linear regression curves for Catalase Activity Test carried out using a HP8453 diode array spectrometer (left) and a NanoDrop Spectrometer (right). The HP8453 diode array test gave 0.1347 O.D. units/min and the NanoDrop Spectrometer gave 0.0132 O.D. units/min. The ten-fold difference in O.D. is due to the ten-fold difference in Optical Paths of the HP8453 diode array (10 mm) and the NanoDrop Spectrometer (1 mm).

For the Diode array test we get ΔOD = 0.1347 AU/min, using Beer-Lambert law we get,

$\Delta OD = \varepsilon \Delta C \rightarrow (0.1347\ AU/min) \div (43.6\ M^{-1}cm^{-1}) = \Delta C = 0.003089\ M\ per\ min$
Using V = 10^{-3} L we get, **$0.003089\ M\ per\ min \times 10^{-3}\ L = 3\ \mu mol\ H_2O_2\ per\ minute$**

For the NanoDrop test we get ΔOD = 0.0132 AU/min, with 10X correction for Optical Path we get,

$\Delta OD = \varepsilon \Delta C \rightarrow (10 \times 0.0132\ AU/min) \div (43.6\ M^{-1}cm^{-1}) = \Delta C = 0.00303\ M\ per\ min$
Using V = 10^{-3} L we get, **$0.00303\ M\ per\ min \times 10^{-3}\ L = 3\ \mu mol\ H_2O_2\ per\ minute$**

Using the definition, 1.0 units will decompose 1.0 µmol H_2O_2 per minute we get,

$(3\ \mu mol\ H_2O_2\ per\ minute) \div (1.0\ \mu mol\ H_2O_2\ per\ minute/unit) = 3.0\ unit$

There are 3 units of catalase in the 1.0 mL volume of the assay. The catalase stock (3.0 mg/mL) was diluted 1000 times, then the solution has 3000 units per mL. Thus the catalase we are using has an activity of 1000 units/mg.

We want to know if a small amount of catalase will deplete the H_2O_2 within a negligible amount of time. The standard 250 µL assay contains 100 µL of 50 mM H_2O_2.

(100 µL X 50 mM H_2O_2) ÷ (1000 µL) = 5.0 mM H_2O_2 = working concentration
5.0 mM H_2O_2 X 10^{-3} L = 5.0 µmol H_2O_2 = amount present in a 1000 µL assay

If the concentration of catalase in the assay is 3.0 units/mL (1/1000 stock) it could deplete 2.0 µmol H_2O_2 in 40 seconds. Using a concentration of 1/100 stock is more than enough to deplete the H_2O_2 within a negligible amount of time.

2.5 Experimental Protocols Summary

For the interpretation of the results it is important to understand that there are two different assays. One is the reaction assay, consisting of the hydroxamide, Myoglobin and Hydrogen peroxide. The other is the Spectrometric assay, which includes the reaction assay, catalase and Griess reagents.

The reaction assays were prepared in such a way that the final concentrations of the hydroxamide, Myoglobin and Hydrogen peroxide are as listed on **Table 2.3**. Equal volumes (100 µL) of the three reagents are mixed and the assay is diluted to 1000 µL. Thus the concentrations of the hydroxamide, Myoglobin and Hydrogen peroxide are decreased by a factor of 10. This means 2.5 mM hydroxamide, 100 µM Myoglobin and 50 mM H_2O_2 become 250 µM hydroxamide, 10 µM Myoglobin and 5 mM H_2O_2 in the reaction assay.

At different points in time, the reaction was stopped using Catalase as a quencher. This is done by having the Catalase ready in a centrifuge tube and adding 100 µL of the reaction assay on top. The volume of Catalase used was 50 µL and the concentration was 300 units/mL. This solution was prepared by diluting the 3000 units/mL stock 10 times. We took 1 volume of Catalase stock and added 9 volumes of Phosphate buffer (pH 7.4). Thus the amount of Catalase added to stop the reaction was,

50 µL (300 units/1000 µL) = 15 Catalase units

In terms of concentration, 50 µL of Catalase are added to 100 µL of reaction assay to give 150 µL of solution. Thus the Catalase is working at a concentration that is 3 times smaller,

50 µL (300 units/1000 µL)] ÷ 150 µL = 100 units/1000 µL

Once the 50 µL of Catalase and the 100 µL of reaction assay are mixed we assume the reaction has stopped completely and we proceed to add the Griess reagents. Because Sulfanilamide is prepared in acidic solution it is best to mix 50 µL of Catalase and the 100 µL of reaction assay before adding the Griess reagents. Otherwise the Catalase might get damaged by the acid in the Sulfanilamide solution. The volume of each of the two Griess reagents used was 50 µL for a total of 100 µL.

Adding all volumes together gives 250 µL for the Spectrometric assay. At this point the concentration if the NO decomposition products have been decreased by a factor of 2.5 or are now 40% compared to the reaction assay concentration.

C1(100 µL) = C2(250 µL)

[C1(100 µL)] ÷ 250 µL = C2 = C1(0.4)

CHAPTER III RESULTS

3.1 Summary of Results

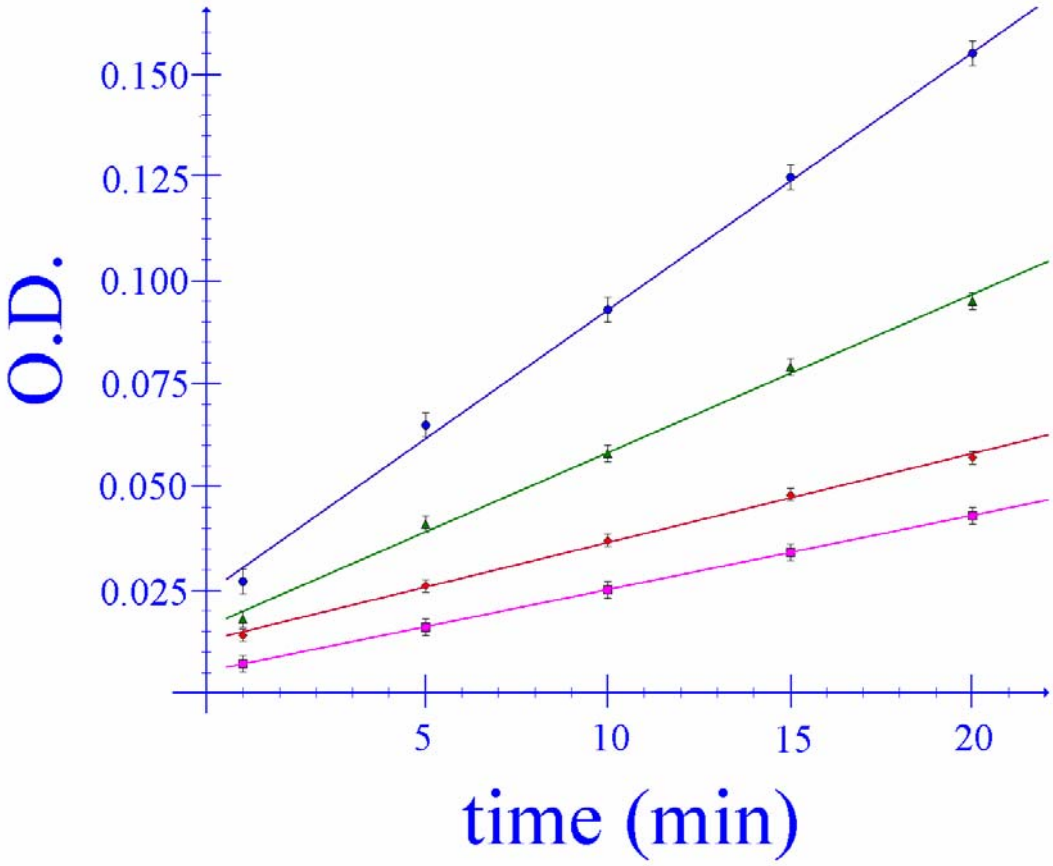

Figure 3.1. Summary of results for NO production rates in O.D. units per minute. The graphs have been overlaid to show how different the slopes are. Data points represent the mean values of two experiments and the error bars are the standard deviation of the mean. These error bars can be takes as a measure of the reproducibility of the O.D. readings.

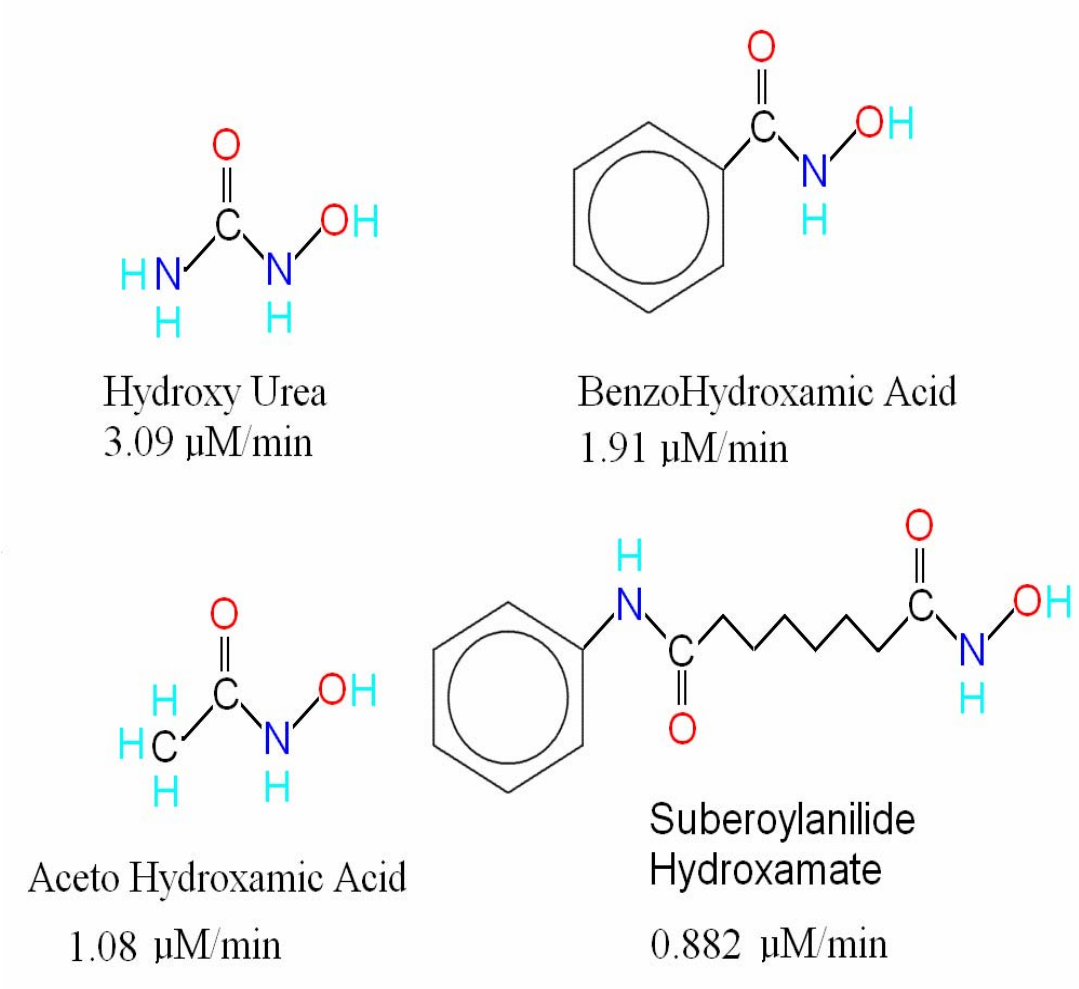

Figure 3.2. Summary of results for NO production rates in µM units per minute showing the structure of the compound. Hydroxy Urea has the fastest NO release rate. SAHA has the slowest NO release rate. The trend is that the larger molecules will have slower oxidation rates. We think that, since the Hydroxamide has to make contact with the HEME group inside Myoglobin, the smaller molecules have easier access to the HEME group. This explanation puts BenzoHydroxamic acid out of place in the sequence and we should consider other factors, such as the stability provided to intermediate ionic species by the presence of a benzene ring.

.

CHAPTER IV DISCUSSION

4.1 Reproducibility of O.D. readings in the NanoDrop

The noise level (Error) in O.D. measurements does not get larger than 5% and all the rates of NO production are reproducible as can be seen from the overlay of trials A+B+C for AcetoHydroxamic Acid in **Figure 4.1**. Sample volumes were as low as 200 µL and using drop sizes of about 40 µL allows about 5 measurements to be done with a single sample. Although the sample cannot be recovered the NanoDrop is a good choice for analyzing reagents that are expensive or in short supply, such as the anticancer drug SAHA.

Even though, measurements were done for a 25 minute time period, only the first 20 minutes were used for computing the rates of NO production. We noted that the reproducibility of the results is quite good during the first 20 minutes of the reaction. After that, the O.D. tends to increase at a much slower rate. We computed the amount of hydroxamide oxidized during a 25 minute period and found it to be between 20 and 30 % of the total amount present at time 0 minutes. This means that after 25 minutes the hydroxamide concentration will drop from 250 to 200 µM. The H_2O_2 concentration will at this point still be quite high. We think the concentration change of the hydroxamide is affecting the reaction rate after a 25 minute period.

We have ruled out the quality of Griess reagents A and B as causes for the drop in the O.D. rate of change because when measured again after 10 minutes, the O.D. of the samples was still the same. This means that the Azo dye produced by the Griess Reagents still retains its spectral properties after a reasonable period of time. [24]

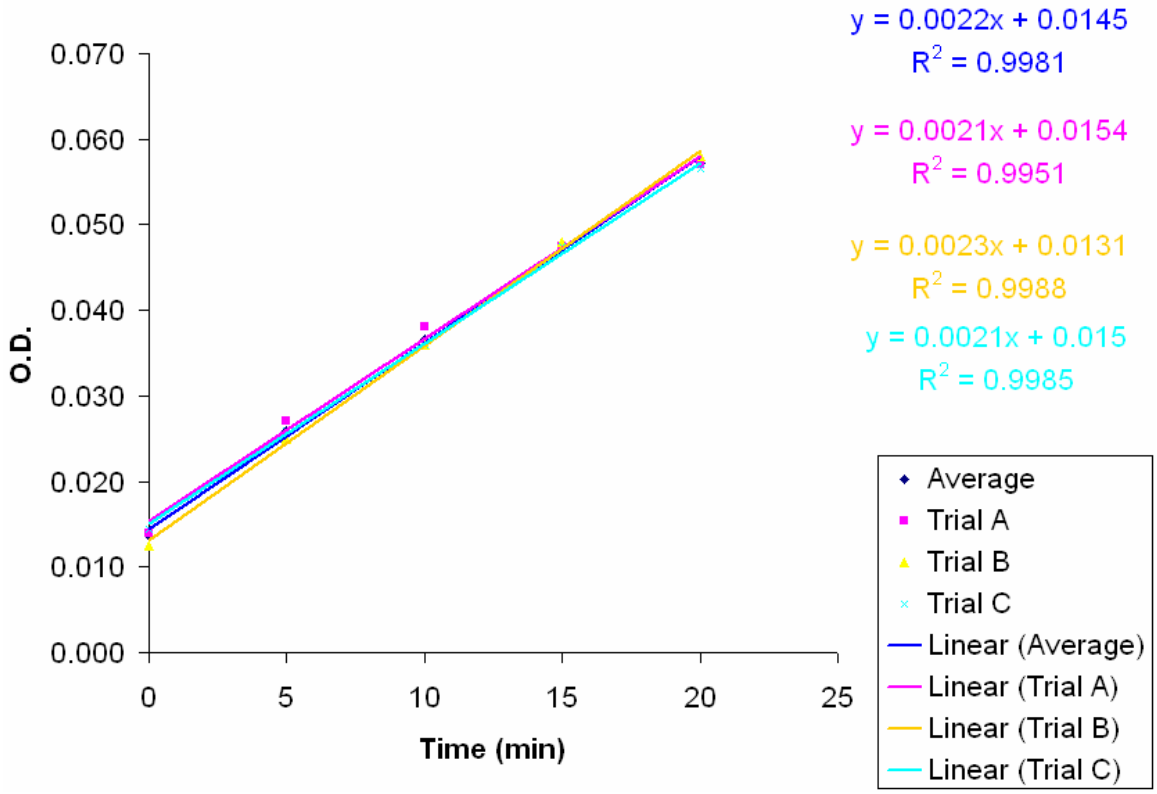

Figure 4.1. Summary of results for NO production rate for AcetoHydroxamic Acid in O.D. units per minute. All measurements were done using the NanoDrop Spectrometer 2000 from Thermo Scientific™. The NO production rate reported in the RESULTS section is the average of these three trials. As can be seen from the overlay of trials A+B+C, the NanoDrop gives reproducible results with acceptable limits of error.

4.2 Reasons for differences in NO production rates

With its role as a pleiotropic regulator, NO is critical to numerous biological processes of interest for cancer research, including macrophage-mediated immunity. [25] However, the role NO in the inmune system is still not well understood. NO has been labeled as a causative agent of DNA damage, yet appears to protect cells against various chemical species generated under oxidative stress. [26]

The link between cancer and the compound NO, was established long before HPCs were identified as anticancer agents.In fact, NO production was not a factor in the

design of SAHA. [27] Thus it was expected that, NO production rate and anticancer activity are not connected, at least according to our results.

Our results indicate that SAHA has the slowest NO production rate despite being the best anticancer drug of the compounds studied. The conclusion is that NO production is not the primary function of SAHA. Its main function is Histone deacetylase inhibition and the relatively slow NO release rate means that SAHA is more resistant to oxidation than the other compounds studied. That would enable SAHA to remain in the body for longer periods of time, requiring fewer doses of the drug to be administered to cancer patients.

CHAPTER V CONCLUSIONS

5.1 Concluding Remarks

Although, controlling the production of NO might be therapeutically desirable, it is still not clear how NO functions in the immune system. For cancer treatment, we probably want localized delivery of a very high concentration of NO. [28] This would cause DNA damage to all cells but would affect cancer cells the most. This is a very simplified explanation and we don't really know all the side effects of NO.

SAHA was not designed with localized delivery of NO in mind. [27] SAHA and its structural analogs were designed to block the active site of zinc-dependent HDACs, with NO production being just a side effect. Low oxidation rates are in fact desirable in prescription drugs because fewer doses of the drug are needed if it does not degrade quickly into unusable byproducts.

Even though, a definite answer as to the mode of action of SAHA is beyond the scope of this thesis, we have managed to establish a working protocol for measuring NO production of reagents that are hard to come by, such as the anticancer drug SAHA.

BIBLIOGRAPHY

1. Allfrey VG, Faulkner R, Mirsky AE,"Acetylation and methylation of histones and their possible role in the regulation of RNA synthesis" *PNAS USA*, **1964**, **51**: 786–794.

2. Zhang Y, Reinberg D. "Transcription regulation by histone methylation: Interplay between different covalent modifications of the core histone tails" *Genes Dev*, **2001**, 15: 2343–2360.

3. Cress WD, Seto E, "Histone deacetylases, transcriptional control, and cancer" *J. Cell Physiol.* **2000**, 184: 1-16.

4. Annamaria H, Beaulieu R, Balicki D, "Histone Tail Modifications and Noncanonical Functions of Histones: Perspectives in Cancer Epigenetics", *Molecular Cancer Therapeutics* **2008**: 7(4), 740-748

5. Jaye M *et al*, "Identification of Novel Isoform-Selective Inhibitors within Class I Histone Deacetylases" *JPET*, **2003**; 307(2): 720-728

6. Arrowsmith CH *et al*, "Human HDAC7 Harbors a Class IIa Histone Deacetylase-specific Zinc Binding Motif and Cryptic Deacetylase Activity" *J. Biol. Chem*, **2008**; 283, 11355-11363

7. Richon V M, Webb Y, Merger R, Sheppard T, Jursic B, Ngo L, Civoli F, Breslow R, Rifkind R A, Marks P A, "Second generation hybrid polar compounds are potent inducers of transformed cell differentiation" *Proc Natl Acad Sci USA,* **1996**: 93,5705–5708.

8. Siegel D S, Zhang X, Feinman R, Teitz T, Zelenetz A, Richon V M, Rifkind R A, Marks P A, Michaeli J, "Hexamethylene bisacetamide induces programmed cell death (apoptosis) and down-regulates BCL-2 expression in human myeloma cells" *Proc Natl Acad Sci USA,* **1998**: 95,162–166.

9. Marks PA, "Discovery and development of SAHA as an anticancer agent", *Oncogene.* **2007**; 26:1351-1356

10. Marks P, Breslow R, "Dimethyl sulfoxide to vorinostat: development of this histone deacetylase inhibitor as an anticancer drug" *Nature Biotechnology* **2007**, 25: 84-90.

1**1**. Arrowsmith CH *et al*, "Human HDAC7 Harbors a Class IIa Histone Deacetylase-specific Zinc Binding Motif and Cryptic Deacetylase Activity" *J. Biol. Chem*, **2008**; 283, 11355-11363

12. Di Marco S *et al*, "Crystal structure of a eukaryotic zinc-dependent histone deacetylase, human HDAC8, complexed with a hydroxamic acid inhibitor" *PNAS USA*, **2004**; 101(42): 15064-15069

13. Su H, Altucci L, You Q, "Competitive or noncompetitive, that's the question: research toward histone deacetylase inhibitors" *Mol. Cancer Ther*, **2008**; 7: 1007

14. Murrell W. "Nitroglycerin as a remedy for angina pectoris" *Lancet* **1879**; 1:113–5

15. Moncada S, Palmer RM, Higgs EA. "Nitric oxide: physiology, pathophysiology, and pharmacology" *Pharmacol Rev* **1991**; 43:109–42

16. Bogdan C, "Nitric Oxide and the immune response", *Nature Immunology.* **2001**; 2:907-916

17. Wink DA, Feelisch M, Vodovotz Y, Fukuto J, Grisham MB, "The chemical biology of NO. An update. Reactive Oxygen Species in Biological Systems. in press; 1998.

18. Weber PC et al, "Structural characterization of nitric oxide synthase isoforms reveals striking active-site conservation", *Nature Structural Biology.* **1999**; 6:233-242

19. Griess JP, *Ber Deutsch Chem Ges*. **1879**, 12: 426

20. Stamler JS, Singel DJ, Loscalzo J, "Biochemistry of nitric oxide and its redox-activated forms" *Science*, **1992**, 258: 1898–1902

21. Parameter™, Griess Reagent Protocol, R&D Systems, Inc. **2010**.

22. Liebhafsky HA,Winslow EH, Spectrometric Determination of Nitrite and Nitric Oxide in Furnace Atmosperes, *Industrial and Engineering Chemistry*. **1939**; 11(4):189-190

23. Tajima GI, Shikama K, "Decomposition of hydrogen peroxide by metmyoglobin: A cyclic formation of the ferryl intermediate " *Int. Journal of Biochem*, **1993**; 25(1): 101-105

24. Fox Jr JB, "Kinetics and mechanisms of the Griess reaction" *Anal. Chem*., **1979**, 51 (9):1493–1502

25. Xu W, Liu LZ, Loizidou M, Ahmed M, Charles IG, "The role of nitric oxide in cancer", *Cell Res.* **2002**; 12(5-6):311-320

26. Jordi J, De la Mata M, "Nitric Oxide and Cancer", *World J Hepatol.* **2010**; 2(9):337-344

27. Richon VM, "Cancer biology: mechanism of antitumour action of vorinostat (suberoylanilide hydroxamic acid), a novel histone deacetylase inhibitor", *British Journal of Cancer.* **2006**; 95: S2-S6

28. Vallance P, Leiper J, "Blocking NO synthesis: how, where and why?", *Nature Reviews Drug Discoveryl.* **2002**; 1:939-950